

Evidence of ferromagnetically coupled Nd^{3+} ion pairs in weakly doped $\text{Nd}:\text{LiYF}_4$ and $\text{Nd}:\text{YVO}_4$ crystals as revealed by high-resolution optical and EPR spectroscopies

O. Guillot-Noël,* V. Mehta,† B. Viana, and D. Gourier

Ecole Nationale Supérieure de Chimie de Paris (ENSCP), Laboratoire de Chimie Appliquée de l'Etat Solide, UMR CNRS 7574, 11 rue Pierre et Marie Curie, 75231 Paris Cedex 05, France

M. Boukhris and S. Jandl

Centre de Recherche en Physique du Solide, Département de Physique, Université de Sherbrooke, Sherbrooke, Quebec, Canada J1K2R1

(Received 22 December 1999)

Electron paramagnetic resonance (EPR) and high-resolution fluorescence spectra of Nd^{3+} ions in weakly doped LiYF_4 and YVO_4 crystals are analyzed. A simple model, based on an effective spin-Hamiltonian approach is proposed to explain the general features of the EPR and optical neodymium spectra in these matrices. Pairs of satellite lines whose intensities grow with neodymium content are observed on each side of the main EPR signals of isolated Nd^{3+} ions. These satellites are assigned to Nd^{3+} - Nd^{3+} ion pairs coupled by magnetic dipolar interaction. The calculated Nd-Nd distances are found to be in good agreement with the Y^{3+} - Y^{3+} distances in LiYF_4 and YVO_4 hosts. The concentration-dependent satellites accompanying the neodymium ${}^4F_{3/2} \rightarrow {}^4I_{9/2}$ transition are quantitatively explained as being due to several types of ferromagnetically coupled pairs of Nd^{3+} ions, each ion of a pair being located at the regular Y^{3+} site with S_4 and D_{2d} point symmetry in LiYF_4 and YVO_4 , respectively. The exchange coupling values J are found in the range $+0.8$ to $+4.9 \text{ cm}^{-1}$. From literature data, it appears that such ferromagnetically coupled Nd^{3+} pairs with $J = +3 \text{ cm}^{-1}$ also quantitatively explain the optical satellite structure in $\text{Nd}:\text{Y}_3\text{Al}_5\text{O}_{12}$ (YAG).

I. INTRODUCTION

Optical transitions of rare-earth ions in condensed matter, even at very low doping levels, often exhibit a multisite character which manifests itself as (i) complex structures in absorption or emission spectra consisting of more $4f$ - $4f$ transitions than expected and/or (ii) inhomogeneously broadened transitions. In particular, it is the case of trivalent neodymium ions in yttrium lithium fluoride (LiYF_4), yttrium orthovanadate (YVO_4), and yttrium aluminate garnet ($\text{Y}_3\text{Al}_5\text{O}_{12}$, YAG), three very important laser crystals.¹⁻⁶ LiYF_4 and YVO_4 matrices are investigated in the present work. LiYF_4 belongs to the scheelite-type structure with space group $I4_1/a(C_{4h}^6)$. The Nd^{3+} ions substitute for trivalent yttrium ions at S_4 point site symmetry. The zircon-type matrix YVO_4 is also tetragonal (space group $I4_1/amd$) and Nd^{3+} ions substitute eightfold coordinated Y^{3+} ions, forming $[\text{YO}_8]$ bisdisphenoid with D_{2d} point site symmetry. Despite these relatively simple crystal structures, which allow only one substitution site for rare-earth ions, a much more complex behavior is observed in optical spectra.⁷⁻¹¹ The optical transitions of isolated Nd^{3+} ions are accompanied by several "satellites" whose intensities grow strongly with neodymium content. It is generally recognized that these extra lines are due to pairs or clusters of ions.

Several experimental works have already been devoted in the past to Nd^{3+} - Nd^{3+} pair spectra in different matrices.¹²⁻²⁰ For example, Pelletier-Allard and Pelletier have performed studies on neodymium satellite structure around the ${}^4I_{9/2} \rightarrow {}^4G_{5/2}$ transition in LaCl_3 using absorption and up-conversion techniques.¹⁶ Additional studies on Nd^{3+} pairs have been reported in LaF_3 by Buisson and co-workers,¹⁷ in

YAlO_3 by Lupei, Lupei, and Georgescu,¹⁴ and in CaF_2 by Basiev *et al.*¹⁸ Energy transfer processes between Nd^{3+} ions, in pairs or in clusters, in CsGd_2F_7 have been discussed by de Barros, Barthem, and Khaidukov.¹⁹ The interaction between pairs of Nd^{3+} ions in CsCdBr_3 was measured by Ramaz, Vial, and Macfarlane using high-resolution spectral hole-burning spectroscopy.²⁰ However, up to now it was not possible to quantify the respective role of exchange interactions and crystal-field effects in pair spectra, as we have done in the present work.

In previous studies on $\text{Nd}:\text{LiYF}_4$,^{7,8} it was shown that for weakly doped crystals, Nd^{3+} ions are inhomogeneously distributed in the host and a coupled pair of Nd^{3+} ions is well isolated from other ions or other pairs. The extra optical lines are assigned to specific types of Nd^{3+} pairs.⁸ However, the interaction mechanism between two ions of a pair is still debated. The same behavior was observed for $\text{Nd}:\text{Y}_3\text{Al}_5\text{O}_{12}$.⁶ For the vanadate host also, the origin of the rich satellite structure, accompanying the transitions of isolated Nd^{3+} ions in unperturbed sites, is still not clear. In all these matrices, these additional optical lines could be due to (i) a fraction of Nd^{3+} ions occupying distorted sites perturbed by neighboring lattice defects such as oxygen vacancies (F -type centers); (ii) a fraction of Nd^{3+} ions occupying distorted sites perturbed by a neighboring Nd^{3+} ion, i.e., there is a mutual crystal-field perturbation between the pair ions; (iii) ferro- or antiferromagnetically coupled pairs of Nd^{3+} ions in unperturbed sites that give rise to exchange (or superexchange) splitting of the isolated ions optical transitions; (iv) a combination of all these mechanisms, where both exchange splitting and crystal-field shifts are responsible for the appearance of the optical satellites.

For Nd:YVO₄ host, a first progress in this area has been made recently by Ermeux *et al.*⁹ These authors performed time-resolved site-selective excitation and emission studies on different Nd:YVO₄ crystals grown by several techniques and/or coming from different origins. These crystals differed by their color and thus by the amount of *F*-type centers. Site-selective spectroscopy showed that, all the samples possess three types of neodymium sites, one of them being largely dominant (site 1) while the other ones (sites 2 and 3) are at least one or two order of magnitude less occupied. These three sites differ by the crystal-field splitting of the neodymium ⁴*F*_{3/2} level which are found to be 18, 25, and 23 cm⁻¹ for sites 1, 2, and 3, respectively. In addition, the optical transitions of Nd³⁺ ions in the dominant site 1 also exhibit a rich satellite structure which could not be interpreted.⁹ From the reproducibility of this satellite structure and its dependence on the Nd³⁺ concentration, it was concluded that this multisite character is possibly due to crystal-field perturbation of neodymium sites by neighboring Nd³⁺ ions [mechanism (ii)]. Alternatively, a recent EPR study of Nd:YVO₄ also showed the existence of a largely dominant neodymium site with *D*_{2d} symmetry, and two minor sites with lower symmetry (*C*_{2v} or *D*₂),¹⁰ which seem to be well correlated with major site 1 and minor sites 2 and 3 found by optical spectroscopy.⁹ In addition, the EPR spectrum of Nd³⁺ ions in dominant site 1 also exhibit concentration dependent satellites resulting from at least three types of Nd³⁺ pairs coupled by magnetic dipole-dipole interactions. It should be emphasized, that the magnetic dipole-dipole interactions between two Nd³⁺ ions forming pairs are of the order of 10⁻² cm⁻¹, which is much lower than the few cm⁻¹ splitting of the optical transitions. In fact, EPR spectrum is not sensitive to a small exchange interaction whereas the dipole-dipole interactions measured by EPR are smaller than the optical linewidth. In other words, EPR and optical spectroscopies are not sensitive to the same interactions. Thus by using EPR and optical spectroscopies separately, we can not unambiguously determine the origin of the complex structure of the optical transitions of Nd³⁺ ions in Nd:YVO₄. It should be stressed that origins of such rare-earth ion pair structures in optical spectra of lightly doped solids still remain an open problem.

In the present work, by using EPR and high-resolution optical spectroscopies, we aim at demonstrating that ground-state exchange interactions rather than crystal-field perturbations of closely spaced Nd³⁺ ions play a dominant role in the optical lines structure in LiYF₄ and YVO₄ matrices.

Recently, Hehlen *et al.* have shown that pairs of rare-earth ions (Yb³⁺) exhibit an intrinsically bistable luminescence resulting from a cooperative effect due to ion-ion coupling within the dimer.²¹ Energy migration between pairs was found to have a degrading effect on bistability and thus only isolated pairs in weakly doped matrix were expected to exhibit bistability.²¹ Therefore, a deeper understanding of ion-ion coupling mechanisms in such pairs is of fundamental interest, and could help to optimize the bistable luminescence effect.

This paper is arranged as follows. After the experimental part in the next section, we present in Sec. III a simple effective spin-Hamiltonian approach which is used to interpret the EPR and optical results. In Sec. IV A, by using EPR

spectroscopy, it is shown that Nd³⁺ ion pairs coupled by magnetic dipolar interaction are present in both LiYF₄ and YVO₄ matrices. Each ion of a pair is localized in regular Y³⁺ sites with *S*₄ and *D*_{2d} point site symmetries for LiYF₄ and YVO₄, respectively. Based on optical measurements of the neodymium ⁴*F*_{3/2}→⁴*I*_{9/2} transition, we show in Sec. IV B that most of the additional lines accompanying this transition are due to ferromagnetically coupled Nd³⁺ pairs, and that crystal-field perturbations of each Nd³⁺ ion by its partner are very weak and cannot explain the observed structures. We also show that this model holds for Nd:Y₃Al₅O₁₂.

II. EXPERIMENTAL PART

YVO₄ single crystals with 0.58% neodymium concentration and LiYF₄ single crystals with 0.33%, 1.2%, and 2% neodymium doping level were grown by the Czochralski method.

EPR measurements were performed at 10 K with a X-band Bruker ESP 300e spectrometer equipped with a variable temperature accessory from Oxford Instrument. The crystals were mounted on a small Perspex sample holder to allow their orientation with respect to the magnetic field. The microwave frequency was measured with a Systron Donner frequency counter.

Low-temperature photoluminescence backscattering measurements were performed using a 514.5 nm Ar ion laser with a double monochromator and conventional photon counting system. Spectra with 0.25 cm⁻¹ resolution were recorded in the 11 350–11 600 cm⁻¹ range with the laser power around 50 mW focused on a 100 μm diameter of the sample. The photoluminescence lines were observed in fresh cut surfaces and from multiple different spots in order to insure that the measurements were not affected by spurious bands due to impurities or surface defects.

III. THE EFFECTIVE SPIN-HAMILTONIAN APPROACH

We describe in this part a simple theoretical background used for the interpretation of electron paramagnetic resonance (EPR) and optical spectra of Nd³⁺ ions pairs. We consider the cases of an isolated Nd³⁺ ion in *S*₄ or *D*_{2d} symmetry (LiYF₄ and YVO₄), an ion pair with mutual crystal-field perturbation and an exchange coupled ion pair.

A. Isolated Nd³⁺ ions and pairs of Nd³⁺ ions with mutual crystal-field perturbation

The Hamiltonian of an isolated Nd³⁺ ion in the unperturbed site of the scheelite and zircon matrices with *S*₄ and *D*_{2d} point symmetry is given by

$$H = H_0 + H_{cf}, \quad (1)$$

where *H*₀ is the free-ion Hamiltonian, including both electron-electron and spin-orbit interaction terms. *H*₀ gives the ^{2S+1}*L*_{*J*} multiplets, in particular the ⁴*I*_{9/2} and ⁴*F*_{3/2} multiplets considered in this work, which are separated by about 11 550 and 11 370 cm⁻¹ in the case of Nd:LiYF₄ and Nd:YVO₄, respectively. The crystal-field Hamiltonian *H*_{cf} lifts the 2*J*+1 degeneracy of the ^{2S+1}*L*_{*J*} states into doubly degenerated states, referred to as Kramers doublets (KD's),

separated by about $10\text{--}10^2\text{ cm}^{-1}$. For the two ${}^4I_{9/2}$ and ${}^4F_{3/2}$ multiplets, the crystal-field interaction gives rise to five and two KD's, respectively (labeled as 1, 2, ...). The residual degeneracy of the KD's can only be lifted by a magnetic field. Therefore, we can attribute to each doublet an effective spin $S = 1/2$. The first two KD's of the ${}^4I_{9/2}$ multiplet being separated by 136 and 110 cm^{-1} in Nd:LiYF₄ and Nd:YVO₄, only the fundamental KD is populated at liquid helium temperature. The two KD's of the ${}^4F_{3/2}$ state are split by 64 and 18 cm^{-1} in LiYF₄ and YVO₄, respectively. The two neodymium ${}^4I_{9/2}(1) \leftrightarrow {}^4F_{3/2}(1)$ transitions occur at $11\,541.0$ and $11\,598.0\text{ cm}^{-1}$ in LiYF₄ and at $11\,364.6$ and $11\,382.6\text{ cm}^{-1}$ in YVO₄, respectively. In the following, we consider only one transition, for example ${}^4I_{9/2}(1) \leftrightarrow {}^4F_{3/2}(1)$. The wave functions $|\phi_0\rangle$ and $|\phi_1\rangle$ associated with the fundamental and the excited KD's can be written as

$$\begin{cases} |\phi_0\rangle = |{}^4I_{9/2}, S_0\rangle, \\ |\phi_1\rangle = |{}^4F_{3/2}, S_1\rangle, \end{cases} \quad (2)$$

where S_0, S_1 are the corresponding effective $\frac{1}{2}$ spins of the two doublets. In the following, the energy splitting between these two KD's is denoted by Δ .

Under an external magnetic field B (EPR measurements), the effective spin Hamiltonian for the ground state $|\phi_0\rangle$, which is the state probed by EPR, can be expressed by the Zeeman term $H_z = \beta\mathbf{B} \cdot \tilde{g} \cdot \mathbf{S}_0$ where \tilde{g} is the g tensor associated with the ground state. The external magnetic field removes the twofold degeneracy of the $|\phi_0\rangle$ state into two singlets at energies $\pm 1/2g(\theta)\beta B$ where the signs $+$ and $-$ correspond to the components $M_S = +1/2$ and $-1/2$ of the effective spin $S = \frac{1}{2}$ and θ is the angle between the direction of the magnetic field and the symmetry axis of the Y³⁺ site. As shown in Fig. 1(a), the EPR transition (selection rules $\Delta S = 0, \Delta M_S = \pm 1$) due to isolated Nd³⁺ ions in unperturbed Y³⁺ sites is expected at energy $g(\theta)\beta B$. If a fraction of Nd³⁺ ions occupy distorted sites, we expect different resonance lines at energies $g'(\theta)\beta B, g''(\theta)\beta B$, etc. ... corresponding to each different site.

For a pair of Nd³⁺ ions with mutual crystal-field perturbation, the crystal field of each ion is modified by its partner, which results in (i) a shift of the ${}^4I_{9/2} \leftrightarrow {}^4F_{3/2}$ transitions and (ii) in a modification of the KD's wave functions, which in turn changes the g -factor values.

B. Exchange coupled pair of Nd³⁺ ions

Let us now consider the Hamiltonian of two coupled Nd³⁺ ions in neighboring sites A and B in both matrices:

$$H_{\text{pair}} = H^A + H^B + V, \quad (3)$$

where H^A and H^B are the Hamiltonian of each individual ion, similar to the one given by Eq. (1). The pairing effect is represented by the interaction term V and by the crystal-field terms included in H^A and H^B , which might reflect mutual crystal-field perturbations of each ion by its partner. For the sake of clarity we neglect this crystal-field effect and consider that the site symmetry remains S_4 or D_{2d} for the two ions of the pair. This hypothesis will be justified *a posteriori* and the small crystal-field effect will be discussed in relation with the experimental results. We thus consider that the fun-

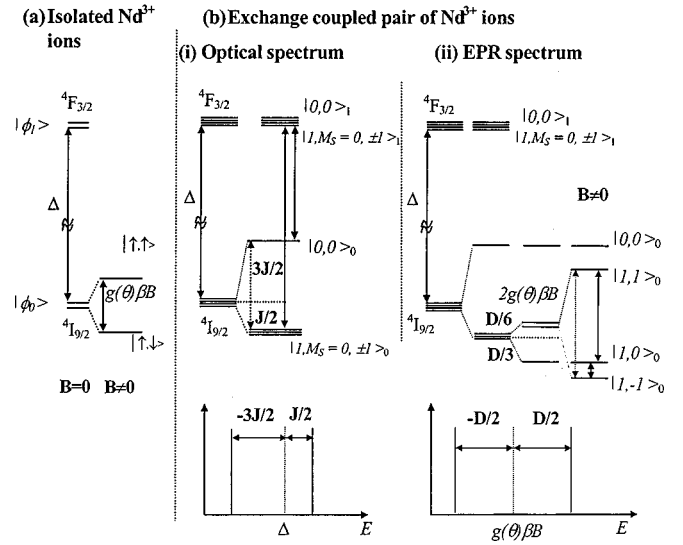


FIG. 1. Energy-level diagram of the neodymium ${}^4I_{9/2}(1) \leftrightarrow {}^4F_{3/2}(1)$ transition for (a) isolated Nd³⁺ ions, the Zeeman interaction being considered only for the fundamental KD and (b) for an exchange coupled pair of Nd³⁺ ions, the exchange (ferromagnetic $J > 0$), dipolar and Zeeman interactions are considered successively. The schematic EPR and optical spectra are also represented. As $J \gg D$ and D is much lower than the optical resolution limit, the dipolar interaction is neglected in the analysis of the optical spectrum.

damental ${}^4I_{9/2}$ KD, the two excited ${}^4F_{3/2}$ KD's of each Nd³⁺ ion forming pair, and their corresponding g factors are that of the isolated Nd³⁺ ions. Knowing that V is of the order of few cm^{-1} (positions of the satellite lines around the main line of isolated Nd³⁺ ions), which is smaller than the energy separation between the closest KD's ($\geq 10^2\text{ cm}^{-1}$), we may consider V as a perturbation acting on the unperturbed states related to the $H^A + H^B$ Hamiltonian. Therefore, it is reasonable to use the states $|\phi_0^A\rangle$ and $|\phi_1^A\rangle$ ($|\phi_0^B\rangle$ and $|\phi_1^B\rangle$) given by Eq. (2) for the $A(B)$ ion to describe the fundamental and excited KD wave functions of the pair. The eigenstates associated with the unperturbed $H^A + H^B$ Hamiltonian are simple products of the form:

$$|\phi_0^A \phi_0^B\rangle_i = |({}^4I_{9/2}, S_0^A), ({}^4I_{9/2}, S_0^B)\rangle_i = |\phi_0^A\rangle |\phi_0^B\rangle_i$$

$$\text{with } i = 1, \dots, 4,$$

$$|\phi_0^A \phi_1^B\rangle_j = |({}^4I_{9/2}, S_0^A), ({}^4F_{3/2}, S_1^B)\rangle_j = |\phi_0^A\rangle |\phi_1^B\rangle_j$$

$$\text{with } j = 1, \dots, 4,$$

$$|\phi_1^A \phi_0^B\rangle_k = |({}^4F_{3/2}, S_1^A), ({}^4I_{9/2}, S_0^B)\rangle_k = |\phi_1^A\rangle |\phi_0^B\rangle_k$$

$$\text{with } k = 1, \dots, 4. \quad (4)$$

The $|\phi_0^A \phi_0^B\rangle_i$ states corresponding to two ions in the ground state are fourfold degenerated as well as the states $|\phi_0^A \phi_1^B\rangle_j$ and $|\phi_1^A \phi_0^B\rangle_k$ corresponding to the excitation of one ion of the pair. The i, j , and k indices label the different degenerated states. The $|\phi_1^A \phi_1^B\rangle_l = |({}^4F_{3/2}, S_1^A), ({}^4F_{3/2}, S_1^B)\rangle_l = |\phi_1^A\rangle |\phi_1^B\rangle_l$ ($l = 1, \dots, 4$) states are neglected because they imply the simultaneous excitation of two Nd³⁺ ions.

The main effects of V in Eq. (3) can be described by three types of matrix elements: (i) elements of the form ${}_i\langle\phi_0^A\phi_0^B|V|\phi_0^A\phi_0^B\rangle_j$ which split the fourfold degenerated ground state of the pair; (ii) elements of the form ${}_i\langle\phi_0^A\phi_1^B|V|\phi_0^A\phi_1^B\rangle_j$ and ${}_i\langle\phi_0^A\phi_0^B|V|\phi_0^A\phi_1^B\rangle_j$, which describe the interaction between one ion in the fundamental KD of the ${}^4I_{9/2}$ multiplet and the other one in one of the ${}^4F_{3/2}$ excited KD's; (iii) elements of the form ${}_i\langle\phi_0^A\phi_1^B|V|\phi_1^A\phi_0^B\rangle_j$ which are responsible for the transfer of excitation from one ion to its neighbor.

In the following, we will consider that the ground-state interaction (i) largely dominates over interactions (ii) and (iii) involving one ion in the excited state. Although these approximations will be discussed in connection with the experimental results, they can be justified as follows. As we will see below, the pair interaction V is of the order of 2 to 5 cm⁻¹ in both matrices. In a simple perturbation approach, the interaction between two states separated by an energy $\Delta \approx 11\,500$ cm⁻¹ (separation between the ${}^4I_{9/2}$ and ${}^4F_{3/2}$ KD's) is of the order of $V^2/\Delta \approx 10^{-3}$ cm⁻¹ for interactions (ii). This value is a lower limit. In a direct EPR measurement on a photoexcited pair of Nd³⁺ ions in LaCl₃ (the ions are in the ${}^4I_{9/2}$ and ${}^4I_{15/2}$ states separated by an energy of $\Delta = 5869$ cm⁻¹), Clemens and Hutchison²² showed that interactions (ii) are of the order of 0.2 to 0.6 cm⁻¹. Such values lie within the resolution limits of our optical spectra. Interactions (ii) can thus be neglected. The off-diagonal matrix elements of the form (iii) are of the order of 10^{-2} – 10^{-1} cm⁻¹.²³ For example, Cone and Meltzer showed that these matrix elements which transfer energy from one Gd³⁺ ion to another in isostructural GdCl₃ and in Gd(OH)₃ compounds vary from 0.01 to 0.44 cm⁻¹ for different ${}^{2S+1}L_J$ multiplets.²³ These values are still within the resolution limit of our optical spectra and thus interaction (iii) can also be neglected in our approach.

Therefore, assuming that the largest contribution to the pair interaction is coming from the ions in their fundamental states, we may write V as the interaction between two identical effective spins $S_0^A = S_0^B = \frac{1}{2}$:

$$V_{\text{eff}} = \mathbf{S}_0^A \cdot \tilde{J} \cdot \mathbf{S}_0^B, \quad (5)$$

where \tilde{J} is a general tensor involving a lot of contributions such as electronic exchange interaction, magnetic dipole-dipole interaction, electric multipole interaction, virtual phonon exchange, and so on. The order of magnitude of all these interactions varies from 0.01 to 10 cm⁻¹ for rare-earth ions.²³

Expression (5) may be rewritten as follows:²⁴

$$\mathbf{S}_0^A \cdot \tilde{J} \cdot \mathbf{S}_0^B = -2J\mathbf{S}_0^A \cdot \mathbf{S}_0^B + \mathbf{d}_{AB}\mathbf{S}_0^A \wedge \mathbf{S}_0^B + \mathbf{S}_0^A \cdot \tilde{D}_{AB} \cdot \mathbf{S}_0^B, \quad (6)$$

where J is a scalar term, \mathbf{d}_{AB} is a polar vector, and \tilde{D}_{AB} is a traceless tensor. The first term $-2J\mathbf{S}_0^A \cdot \mathbf{S}_0^B$ of Eq. (6) is known as the Heisenberg exchange interaction. Both two-center or direct exchange, and higher-order multicenter or superexchange processes involving the ligands may contribute to J . As each ion of the pair is located in an undistorted site with S_4 or D_{2d} point symmetry, they are related by an inversion symmetry and thus the term $\mathbf{d}_{AB}\mathbf{S}_0^A \wedge \mathbf{S}_0^B$ vanishes by symmetry. Furthermore, since Nd-Nd distances in a pair (the Y³⁺-Y³⁺ distances vary from 3.72 to 8.19 Å in LiYF₄

and from 3.89 to 7.12 Å in YVO₄) are larger than the ion size (1.1 Å), we may describe the dipolar interaction \tilde{D}_{AB} by a pure magnetic dipole-dipole interaction between the two effective spins S_0^A and S_0^B .

The effective spin-Hamiltonians H_0^{eff} for the ground level $|\phi_0^A\phi_0^B\rangle_{i=1,\dots,4}$ and H_1^{eff} for the excited level $|\phi_q^A\phi_{r \neq q}^B\rangle_{j=1,\dots,4}$ (with $q, r = 0$ or 1) of the Nd³⁺-Nd³⁺ pair can thus be written as

$$H_0^{\text{eff}} = -2J\mathbf{S}_0^A \cdot \mathbf{S}_0^B + \mathbf{S}_0^A \tilde{D}_{AB} \mathbf{S}_0^B, \quad (7)$$

$$H_1^{\text{eff}} = \Delta, \quad (8)$$

respectively. As stated before, the pair interaction has been neglected for the excited level.

The fundamental and excited levels are fourfold degenerated. In the individual effective spin $\{|S^A, M_S^A, S^B, M_S^B\rangle\}$ representation, each state can be described by the z components $M_S^A = \pm \frac{1}{2}$, $M_S^B = \pm \frac{1}{2}$ of the effective spins S^A, S^B . The ground and excited states of the pair may thus be written as follows

$$\begin{aligned} |\phi_0^A\phi_0^B\rangle &= |\uparrow, \uparrow\rangle_0, |\uparrow, \downarrow\rangle_0, |\downarrow, \uparrow\rangle_0 \text{ or } |\downarrow, \downarrow\rangle_0, \\ |\phi_0^A\phi_1^B\rangle &= |\uparrow, \uparrow\rangle_1, |\uparrow, \downarrow\rangle_1, |\downarrow, \uparrow\rangle_1 \text{ or } |\downarrow, \downarrow\rangle_1. \end{aligned} \quad (9)$$

We can define a total effective spin S characterized by $\mathbf{S} = \mathbf{S}^A + \mathbf{S}^B$, with $|S^A - S^B| \leq S \leq S^A + S^B$. The two possible values of the total spin are $S = 0$ (with $M_S = 0$) and $S = 1$ (with $M_S = 1, 0, -1$). In the total effective spin $\{|S, M_S\rangle\}$ representation, the ground and excited states of the pair become

$$\begin{aligned} |\phi_0^A\phi_0^B\rangle &= |1, 1\rangle_0, |1, -1\rangle_0, |1, 0\rangle_0 \text{ or } |0, 0\rangle_0, \\ |\phi_0^A\phi_1^B\rangle &= |1, 1\rangle_1, |1, -1\rangle_1, |1, 0\rangle_1 \text{ or } |0, 0\rangle_1, \end{aligned} \quad (10)$$

with the following well-known relation between the two representations:

$$\begin{aligned} |1, 1\rangle &= |\uparrow, \uparrow\rangle, \\ |1, -1\rangle &= |\downarrow, \downarrow\rangle, \\ |1, 0\rangle &= \frac{1}{\sqrt{2}}(|\uparrow, \downarrow\rangle + |\downarrow, \uparrow\rangle), \\ |0, 0\rangle &= \frac{1}{\sqrt{2}}(|\uparrow, \downarrow\rangle - |\downarrow, \uparrow\rangle). \end{aligned} \quad (11)$$

In the total effective spin representation, the effective spin Hamiltonian in Eq. (7) becomes

$$H_0^{\text{eff}} = -J \left(S(S+1) - \frac{3}{2} \right) + \frac{D}{2} \left(S_z^2 - \frac{1}{3} S(S+1) \right) \quad (12)$$

with²⁵

$$D = 0.325g^2(3 \cos^2(\theta) - 1)R^{-3} \quad (13)$$

for a pure magnetic dipole-dipole interaction. Here $D > 0$ is given in cm^{-1} , R (in \AA) is the Nd^{3+} - Nd^{3+} distance, and θ is the angle between the direction of the magnetic field and that of the pair axis.

The exchange term in Eq. (12) splits the fourfold degenerated ground state $|\phi_0^A \phi_0^B\rangle_{i=1, \dots, 4}$ into a singlet state $|0,0\rangle_0$ at energy $3J/2$ and into a triplet $|1, M_S=0, \pm 1\rangle_0$ at energy $-J/2$. The dipolar interaction splits the triplet state into a singlet state $|1,0\rangle_0$ at energy $-D/3$ and in a doublet $|1, \pm 1\rangle_0$ at energy $D/6$. The resulting energy level diagram for a coupled Nd^{3+} ion pair is shown in Fig. 1(b).

As the shortest Y^{3+} - Y^{3+} distances R vary from 3.72 to 8.19 \AA in LiYF_4 and 3.89 to 7.12 \AA in YVO_4 , the D values given by Eq. (13) will be of the order of 10^{-2}cm^{-1} . This magnetic dipolar interaction is thus unresolved in our optical spectra (resolution around 0.25cm^{-1}). Hence, as shown in Fig. 1(b), the optical spectrum (absorption and emission) of a ground-state exchange coupled pair should be a doublet of satellites at photon energies $\Delta + J/2$ and $\Delta - 3J/2$, disymmetrically placed around the isolated ion transition at energy Δ [Fig. 1(b)]. The doublet splitting is $2J$ with the exchange interaction J positive (negative) for ferromagnetically (antiferromagnetically) coupled ions. Figure 1(b) represents the case of a ferromagnetically coupled pair. It is important to emphasize that this behavior is expected only if the ground-state exchange splitting is the unique pair interaction as we have assumed. In the case of an additive crystal-field perturbation of an ion by its partner, the transitions should occur at energies $\Delta' + J/2$ and $\Delta' - 3J/2$. In the case of an excited exchange interaction in addition to the ground-state exchange splitting, the spectra should significantly deviate from the simple picture described in Fig. 1(b).

By applying an external magnetic field B (EPR measurements), the twofold degeneracy of the $|1, \pm 1\rangle_0$ states is lifted into two singlets at energies $\pm g(\theta)\beta B$. The singlet $|1,0\rangle_0$ state remains unaffected. The EPR pair transitions (selection rules $\Delta S=0$, $\Delta M_S = \pm 1$) are expected at energies $g(\theta)\beta B \pm D/2$ [Fig. 1(b)]. Thus the EPR spectrum of a coupled Nd^{3+} ion pair will be a doublet of satellites symmetrically placed around the isolated ion line at energy $g(\theta)\beta B$.

IV. EXPERIMENTAL RESULTS AND DISCUSSION

A. EPR results

The principal EPR signals, observed in the range 180–350 mT and 200–375 mT for $\text{Nd}:\text{LiYF}_4$ and $\text{Nd}:\text{YVO}_4$ (Fig. 2), are attributed to isolated Nd^{3+} ions located at the undistorted Y^{3+} sites with S_4 and D_{2d} point symmetry, respectively. They are composed of one intense central line due to even neodymium isotopes $^{142,144,146}\text{Nd}$ with nuclear spins $I=0$ (natural abundance of 79.5%) and a hyperfine pattern composed of two sets of eight lines for the two odd neodymium isotopes ^{143}Nd and ^{145}Nd with nuclear spins $I=7/2$ (natural abundance of 12.2% and 8.3%, respectively). The relative intensities of the lines are proportional to the natural abundance of the isotopes. For both matrices, the line positions are described by an axial spin-Hamiltonian with an effective spin $S=\frac{1}{2}$.^{10,26,27} The g factors and hyperfine structure constants are determined and are listed in Table I.

For $\text{Nd}:\text{YVO}_4$, two weaker signals (not shown) are observed at higher magnetic fields. From their g factors, they

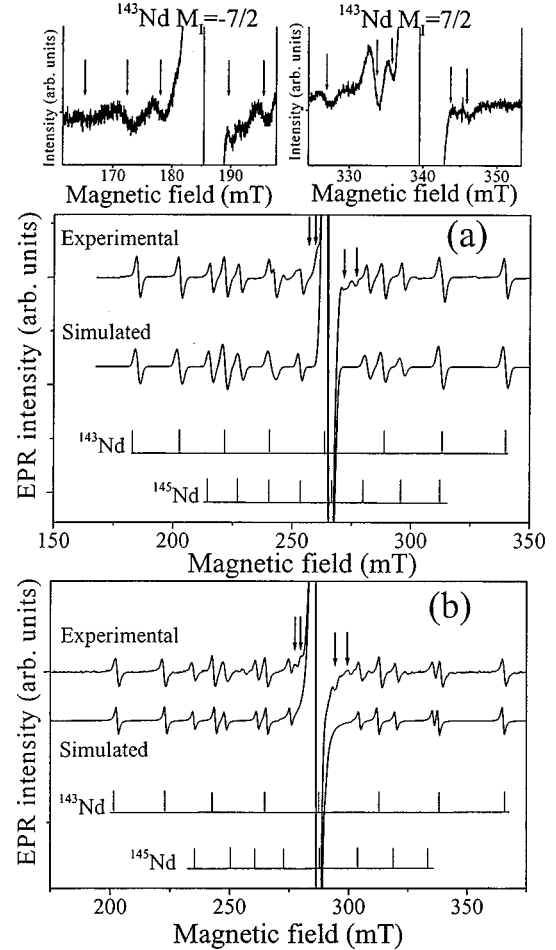


FIG. 2. Experimental and simulated EPR spectra of (a) 0.33% $\text{Nd}:\text{LiYF}_4$ and (b) 0.58% $\text{Nd}:\text{YVO}_4$ at 10 K with $B \perp c$. Concentration-dependent satellites are indicated by arrows. The insets show the ^{143}Nd hyperfine $M_1 = \pm 7/2$ transitions in LiYF_4 , with the concentration-dependent satellites represented by arrows.

were assigned to a small fraction (around 0.1%) of Nd^{3+} ions in distorted sites with symmetry lower than D_{2d} .¹⁰

Besides the main EPR signals of isolated Nd^{3+} ions, several pairs of satellites appear on each side of the central line (indicated by arrows in Fig. 2). The satellites are not seen at very low doping levels and their intensities increase with neodymium concentration. Figure 2 shows the comparison between the simulated and experimental EPR spectra of 0.33% $\text{Nd}:\text{LiYF}_4$ and 0.58% $\text{Nd}:\text{YVO}_4$ samples, recorded with external field B perpendicular to the crystallographic c axis. The hyperfine patterns are calculated up to second order

TABLE I. Spin-Hamiltonian parameters for Nd^{3+} ions in LiYF_4 , and YVO_4 .

		$\text{Nd}:\text{LiYF}_4$	$\text{Nd}:\text{YVO}_4$
g_{\parallel}		1.986 ± 0.003	0.915 ± 0.004
g_{\perp}		2.553 ± 0.002	2.361 ± 0.003
$A_{\parallel} (10^{-4} \text{cm}^{-1})$	^{143}Nd	198.4 ± 0.1	112.1 ± 0.3
	^{145}Nd	123.0 ± 0.3	70 ± 1
$A_{\perp} (10^{-4} \text{cm}^{-1})$	^{143}Nd	265 ± 2	256.9 ± 0.3
	^{145}Nd	164.0 ± 0.6	159.3 ± 0.4

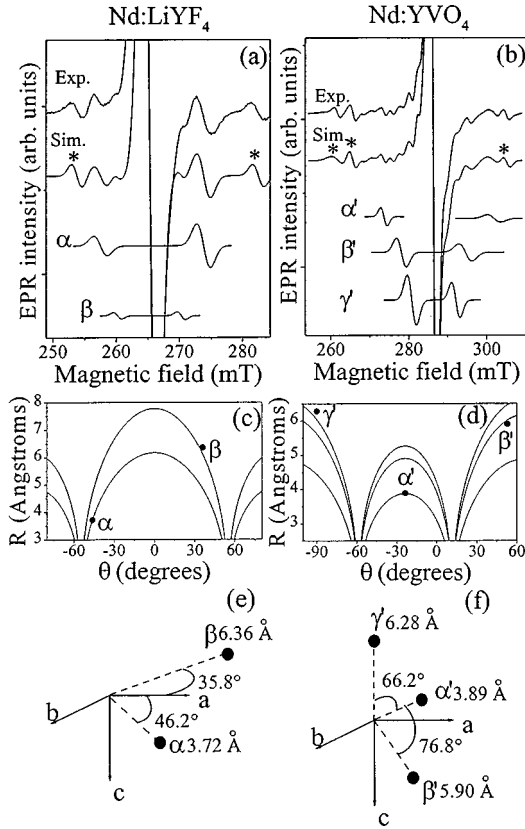


FIG. 3. Expanded view of the central part of the experimental and simulated central EPR line at 10 K with $B \perp c$ of (a) 1.2% Nd:LiYF₄ and (b) 0.58% Nd:YVO₄. Plot of the distance R versus the angle θ , using experimental D values for Nd³⁺ ion pairs in (c) Nd:LiYF₄, and (d) Nd:YVO₄. The circles represent the (θ, R) values from the crystal structure of LiYF₄ and YVO₄ compatible with the experimental curves. Representation of the crystallographic pairs of Nd³⁺ ions at Y³⁺ sites (e) α and β in LiYF₄ and (f) α' , β' , and γ' in YVO₄.

in perturbation and agree satisfactorily with the experimental spectra except for the existence of the concentration dependent lines (shown by arrows) flanking the central line of even isotopes. Moreover, the hyperfine lines also show a similar concentration-dependent satellite structure. This can be observed from the two insets in Fig. 2(a) showing, $M_I = \pm 7/2$ hyperfine lines of ¹⁴³Nd in LiYF₄. These extra lines must thus be analyzed in terms of pairs of interacting Nd³⁺ ions instead of forbidden hyperfine transitions. Satellites around the intense central lines are due to pairs of the type ^{even}Nd³⁺-^{even}Nd³⁺ of two neodymium nuclei with zero nuclear spin $I=0$. Satellites flanking the hyperfine lines, for example those shown in Fig. 2(a), belong to pairs of the type ¹⁴³Nd³⁺-^{even}Nd³⁺. As the splitting between the satellites are of the order of 10^{-2} cm⁻¹, they are due to magnetic dipolar interactions between $S = \frac{1}{2}$ effective spins of neighboring Nd³⁺ ions. Figure 3 shows the central part of the experimental EPR spectra of 1.2% Nd:LiYF₄ and 0.58% Nd:YVO₄ samples along with the fitted spectra using Gaussian lineshape functions. Two pairs of satellites with zero-field splitting D of 0.018 and 0.011 cm⁻¹ are identified [Fig. 3(a)] for Nd:LiYF₄ while for Nd:YVO₄ three pairs of satellite lines are identified with D values of 0.031, 0.018, and 0.012 cm⁻¹ [Fig. 3(b)]. The transitions indicated by stars in Figs. 3(a) and 3(b) are hyperfine lines.

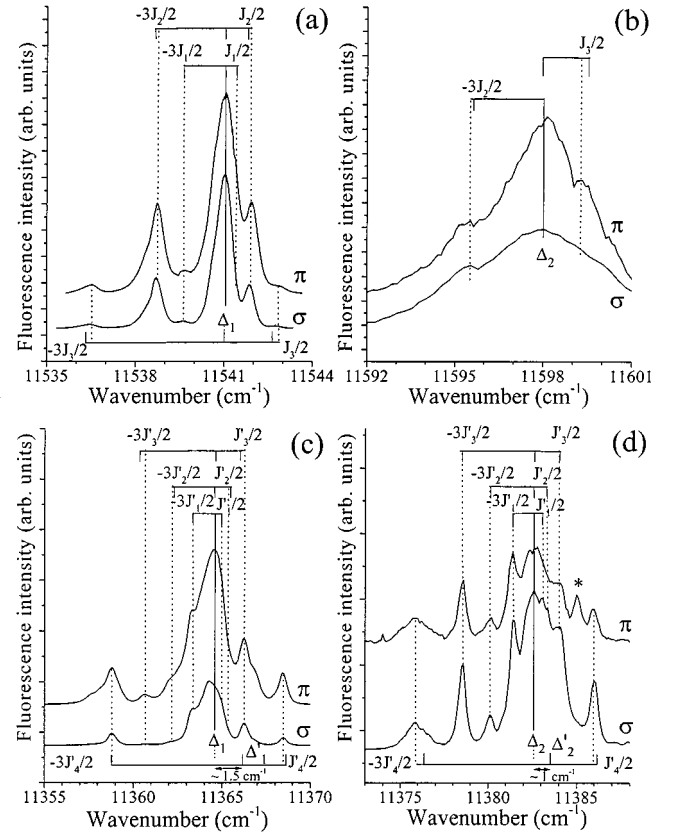


FIG. 4. Expanded views of the π and σ polarized ${}^4F_{3/2} \rightarrow {}^4I_{9/2}$ transitions in 2% Nd:LiYF₄ [(a) and (b)] and in 0.58% Nd:YVO₄ [(c) and (d)]. The emitting state is ${}^4F_{3/2}(1)$ in (a) and (c), and ${}^4F_{3/2}(2)$ in (b) and (d). The isolated ion transitions are represented by full lines while the satellite lines are indicated by discontinuous lines. The calculated positions of the satellites assuming ferromagnetic exchange interaction between Nd³⁺ ion pairs are shown by small solid sticks. For the vanadate host, the transition indicated by a star in (d) is assigned to Nd³⁺ ions in distorted sites referred to as site 2 by Ermeneux *et al.*⁸ For 2% Nd:LiYF₄, three pair lines with $J_1 = 0.8(4)$ cm⁻¹, $J_2 = 1.6(1)$ cm⁻¹, and $J_3 = 3.1(5)$ cm⁻¹ are found. For 0.58% Nd:YVO₄, four pairs with $J'_1 = 0.8(6)$ cm⁻¹, $J'_2 = 1.6(4)$ cm⁻¹, $J'_3 = 2.7(5)$ cm⁻¹, and $J'_4 = 4.9(0)$ cm⁻¹ values are identified.

For both matrices, the line doublets are symmetrically placed around the central line irrespective of the orientation of the magnetic field with respect to the crystallographic axes. This indicates that neodymium ions involved in pairs have the same g values as the isolated neodymium ions, and are located in the same crystal-field environment with S_4 or D_{2d} point site symmetry. Assuming a dipole-dipole magnetic interaction, the allowed orientation θ of the pair axis with respect to the magnetic field and the distance R between the two interacting ions can be determined by plotting $R = f(\theta)$ from Eq. (13) using the experimental D values. Figs. 3(c) and 3(d) present such plots for Nd:LiYF₄ and Nd:YVO₄, respectively. From the crystal structure of LiYF₄, two pairs α and β of Nd³⁺ ions located at Y³⁺ ions site give (θ, R) values [solid circles in Fig. 3(c)] in good agreement with the experimental curves. These Nd³⁺-Nd³⁺ pairs are shown in Fig. 3(e). The α pair is oriented at 46.2° from a (or b) axis

TABLE II. Experimental and calculated positions of the satellites around ${}^4F_{3/2} \rightarrow {}^4I_{9/2}$ transitions of neodymium in 2% Nd:LiYF₄ and 0.58% Nd:YVO₄.

${}^4F_{3/2} \rightarrow {}^4I_{9/2}$ transitions (cm ⁻¹)	Nd:LiYF ₄			${}^4F_{3/2} \rightarrow {}^4I_{9/2}$ transitions (cm ⁻¹)	Nd:YVO ₄				
	Experimental satellite positions (cm ⁻¹)	Calculated satellite positions			Experimental satellite positions (cm ⁻¹)	Calculated satellite positions			
		$J_1=0.8(4)$ (cm ⁻¹)	$J_2=1.6(1)$ (cm ⁻¹)	$J_3=3.1(5)$ (cm ⁻¹)		$J'_1=0.8(6)$ (cm ⁻¹)	$J'_2=1.6(4)$ (cm ⁻¹)	$J'_3=2.7(5)$ (cm ⁻¹)	$J'_4=4.9(0)$ (cm ⁻¹)
	11 536.5			11 536.3	11 358.8				11 357.3
	11 538.7		11 538.6		11 360.7				11 360.5
	11 539.7	11 539.7			11 362.0		11 362.1		
11 541.0					11 363.3	11 363.3			
	11 541.4	11 541.4		11 364.6					
	11 541.9		11 541.8		11 365.0	11 365.0			
	11 542.8			11 542.6	11 365.3		11 365.4		
					11 366.2			11 366.0	
					11 368.4				11 367.1
					11 375.8				11 375.3
	11 595.5		11 595.6		11 378.6			11 378.5	
					11 380.1		11 380.1		
11 598.0					11 381.4	11 381.3			
				11 382.6					
					11 383.1	11 383.0			
	11 599.3		11 599.5		11 383.4		11 383.4		
					11 384.0			11 384.0	
					11 386.0				11 385.1

with $R=3.72$ Å and the β pair is oriented at 35.8° from a (or b) axis with $R=6.36$ Å. For Nd:YVO₄, three Nd³⁺-Nd³⁺ pairs α' , β' and γ' , shown in Fig. 3(f), give (θ, R) values [solid circles in Fig. 3(d)] compatible with the experimental curves. The α' pair is oriented at 66.2° from the c axis with $R=3.89$ Å. The β' pair is oriented at 76.8° from α' pair with $R=5.90$ Å and the γ' pair is along c axis with $R=6.28$ Å.

It is worth noticing that the axial g tensors of Nd³⁺ ions involved in pairs and isolated Nd³⁺ ions are identical, which indicate that both kinds of neodymium experience the same crystal field. This lack of evident crystal-field distortion indicates that the exchange splitting mechanism rather than crystal-field perturbation of closely spaced Nd³⁺ ions are responsible for the structure of optical satellites in these matrices.

B. High-resolution fluorescence spectroscopy

Figure 4 shows the π and σ polarized emission spectra of 2% Nd:LiYF₄ and 0.58% Nd:YVO₄ samples, at 22 and 10 K, respectively, observed in the vicinity of the two ${}^4F_{3/2} \rightarrow {}^4I_{9/2}$ transitions. The positions of the emissions from the two ${}^4F_{3/2}$ KD's of isolated Nd³⁺ ions in unperturbed sites are labeled as Δ_1 and Δ_2 . For both samples, a complex satellite structure whose intensity depends on Nd³⁺ content is observed around these two main lines. For the vanadate host, the transition indicated by a star in Fig. 4(d) is assigned to Nd³⁺ ions in distorted sites labeled as site 2 by Ermenoux *et al.*⁹

For both samples, the satellite patterns are very similar. All the satellite lines (indicated by discontinuous lines in Fig. 4) are grouped within ± 10 cm⁻¹ around the parent lines.

They extend farther away on the low-energy side of the parent line. Moreover, all these additional optical lines seem to form pairs, the two pair lines being disymmetrically placed around the main lines at Δ_1 and Δ_2 . This suggests that these pairs of satellites could be due to exchange coupled Nd³⁺ ions with a positive value of the coupling constant J . In fact, the positions of all the main satellite lines in Fig. 4 can be explained by attributing them to weakly ferromagnetically coupled pairs of Nd³⁺ ions characterized by different J values. As described in Sec. III B, for an exchanged coupled pair, a doublet of satellites is expected at energies $\Delta - 3J/2$ and $\Delta + J/2$ [see Fig. 1(b)]. Table II lists the experimental and calculated positions of the satellite lines accompanying the two neodymium ${}^4F_{3/2} \rightarrow {}^4I_{9/2}$ transitions. The calculated positions are also shown in Fig. 4 by small solid sticks. As can be observed from Table II and Fig. 4, the calculated positions of the satellites are in good agreement with the experimental positions for Nd:LiYF₄. The pairs are characterized by $J_1 = +0.8(4)$ cm⁻¹, $J_2 = +1.6(1)$ cm⁻¹, and $J_3 = +3.1(5)$ cm⁻¹. The situation is much less clear for the line at Δ_2 , since the latter was found to be very broad in our experiments. Nevertheless, two satellites at $-3J_1/2$ and $J_3/2$ corresponding to the J_1 and J_3 pairs can be detected. For Nd:YVO₄, the calculated positions are also in good agreement with the pairs characterized by $J'_1 = +0.8(6)$ cm⁻¹, $J'_2 = +1.6(4)$ cm⁻¹, and $J'_3 = +2.7(5)$ cm⁻¹ ferromagnetic interactions. This agreement holds for both emission lines at Δ_1 and Δ_2 [Figs. 4(c) and 4(d)]. However, small discrepancies around 1 cm⁻¹ are observed for the pair with $J'_4 = +4.9(0)$ cm⁻¹. These discrepancies could be due to small crystal-field perturbations induced by one ion on its partner,

TABLE III. Experimental and calculated positions of two satellites around ${}^4F_{3/2}(1) \rightarrow {}^4I_{9/2}(1)$ transition of neodymium in 1% $\text{Nd}:\text{Y}_3\text{Al}_5\text{O}_{12}$.

${}^4F_{3/2}(1) \rightarrow {}^4I_{9/2}(1)$ transition (cm^{-1}) ^a	Experimental satellite positions (cm^{-1}) ^a	Calculated satellite positions $J_1'' = 3$ (cm^{-1})
11 425.5 (<i>N</i>)	11 420.5 (M_1)	11 421
	11 426.5 (M_2)	11 427

^aAfter Lupei *et al.*, Ref. 6.

as described in Sec. III A. The agreement is much better if the pair is centered at $\Delta'_1 = \Delta_1 + 1.5 \text{ cm}^{-1}$ [Fig. 4(c)] and at $\Delta'_2 = \Delta_2 + 1 \text{ cm}^{-1}$ [Fig. 4(d)]. In this case the crystal-field perturbation of the pair is only about 10% of the exchange interaction. It is important to notice that both ${}^4F_{3/2}(1) \rightarrow {}^4I_{9/2}(1)$ and ${}^4F_{3/2}(2) \rightarrow {}^4I_{9/2}(1)$ transitions exhibit the same satellite structure with exactly the same J values. This demonstrates that since the ground state is common to these two transitions, the exchange interaction is a ground-state exchange interaction.

It may be mentioned that this simple model of pair interactions, can be used to interpret the spectra of rare-earth ion pairs in other matrices. For example, previous optical studies on Nd^{3+} ions in $\text{Y}_3\text{Al}_5\text{O}_{12}$ have shown the presence of few satellites whose relative intensities depend on the dopant concentration.^{6,28} These satellites are assigned to the near-neighbor pairs of Nd^{3+} ions in regular unperturbed dodecahedral c sites with D_2 point site symmetry of the garnet lattice.⁶ Table III gives the experimental positions of two satellites lines (referred to as M_1 and M_2 lines in Ref. 6) observed in the neodymium ${}^4I_{9/2}(1) \rightarrow {}^4F_{3/2}(1)$ transmission spectra, recorded at 30 K for 1% $\text{Nd}:\text{Y}_3\text{Al}_5\text{O}_{12}$ sample. These satellites can be attributed to a $\text{Nd}^{3+}\text{-Nd}^{3+}$ pair characterized by a ferromagnetic interaction $J_1'' = +3.0 \text{ cm}^{-1}$. The discrepancy with the experimental positions is only 0.5 cm^{-1} .

Looking at the J values in Table II, it can be noticed that as J increases, there is an increasing discrepancy between the calculated and experimental positions due probably to an increase in the mutual crystal field perturbation of the two coupled Nd^{3+} ions. In both LiYF_4 and YVO_4 matrices, the agreement is almost perfect for pairs with $J < 1 \text{ cm}^{-1}$. Pairs with J in the range 1.6 to 3 cm^{-1} are characterized by discrepancies of the order of 0.1 to 0.2 cm^{-1} . This discrepancy reaches around 1 cm^{-1} for the more strongly coupled pair with $J = 4.9 \text{ cm}^{-1}$ in YVO_4 . Therefore, the coupling constant J could be correlated with $\text{Nd}^{3+}\text{-Nd}^{3+}$ distances in these matrices. For the zero-field splitting D measured from EPR spectra, this correlation is evident as D is proportional to R^{-3} . However, a deeper study of the nature of the interactions represented by the J term should be done to correlate the pairs identified in the optical spectra with the pairs seen by EPR spectroscopy.

V. CONCLUSION

In this paper, a general model based on an effective spin-Hamiltonian approach is developed to explain the concentration dependent neodymium satellite structure observed in EPR and optical spectra of weakly doped LiYF_4 and YVO_4 laser hosts. The model considers only the interaction between the lowest fundamental Kramers doublets of two identical Nd^{3+} ions. EPR studies provide evidence for the existence of Nd^{3+} ions coupled by magnetic dipolar interaction. Each ion of a pair is localized in the undistorted Y^{3+} site with S_4 and D_{2d} point site symmetry for LiYF_4 and YVO_4 matrices, respectively. Based on the proposed model, the calculated additional optical lines, attributed to ferromagnetically coupled pairs, satisfactorily explain the main features of the observed satellite structure accompanying the two ${}^4F_{3/2} \rightarrow {}^4I_{9/2}$ transitions. For $\text{Nd}:\text{LiYF}_4$, at least three different pairs have been identified, characterized by ferromagnetic J interactions of $+0.8(4) \text{ cm}^{-1}$, $+1.6(1) \text{ cm}^{-1}$, and $+3.1(5) \text{ cm}^{-1}$. For $\text{Nd}:\text{YVO}_4$, at least four pairs are identified characterized by J values of $+0.8(6) \text{ cm}^{-1}$, $+1.6(4) \text{ cm}^{-1}$, $+2.7(5) \text{ cm}^{-1}$, and $+4.9(0) \text{ cm}^{-1}$. The good agreement between the calculated and the experimental results demonstrates that ferromagnetic exchange interactions rather than crystal-field perturbations of closely spaced Nd^{3+} ions play a dominant role in the structure of the optical lines in LiYF_4 and YVO_4 . Small crystal-field perturbations of about 1 cm^{-1} are observed for pairs with high J values (4.9 cm^{-1}). However, crystal-field effects are very small (compared to $11\,300 \text{ cm}^{-1}$ energy of ${}^4F_{3/2} \rightarrow {}^4I_{9/2}$ transition) and cannot explain the observed structure.

Moreover, it appears that this scheme could be applied to other matrices where Nd^{3+} pairs have already been seen. In the $\text{Nd}:\text{Y}_3\text{Al}_5\text{O}_{12}$ (YAG) laser host, some satellites can also be attributed to ferromagnetically coupled pairs. For the other zircon-type hosts $\text{Nd}:\text{YAsO}_4$, $\text{Nd}:\text{YPO}_4$, we have recently observed such concentration dependent satellite structure which can also be characterized by this model. All these experiments are currently in progress.

However, a deeper investigation of the nature of the interactions represented by the positive J term should be done to correlate the ferromagnetically coupled pairs identified by optical spectra to the magnetic dipolar coupled pairs seen by EPR spectroscopy.

ACKNOWLEDGMENTS

The authors are grateful to the Direction Générale de l'Armement (DGA, France) and NATO for financial support. We wish to thank Dr. B. Ferrand (LETI-CEA) and Dr. J. Y. Gesland (Groupe de Cristallogénèse, Université du Maine, Le Mans) for providing 0.58% $\text{Nd}:\text{YVO}_4$ and 0.33% , 1.2% , and 2% $\text{Nd}:\text{LiYF}_4$ crystals, respectively. We are indebted to Professor R. Moncorgé (Laboratoire de Spectroscopie Atomique, ISMRA, Caen) for fruitful discussions.

- * Author to whom correspondence should be addressed. Electronic address: oguillot@enscp.jussieu.fr
- † On leave from Kalindi College, University of Delhi, East Patel Nagar, New Delhi-110008, India.
- ¹M. J. Weber, in *Methods of Experimental Physics*, edited by C. L. Tang (Academic, New York, 1979), Vol. 15, p. 167.
- ²T. M. Pollak, W. F. Wing, R. J. Grasso, E. P. Chicklis, and H. P. Janssen, *IEEE J. Quantum Electron.* **QE-18**, 159 (1982).
- ³D. G. Matthews, J. R. Boon, R. S. Conroy, and B. D. Sinclair, *J. Mod. Opt.* **43**, 1079 (1996).
- ⁴B. H. T. Chai, G. Loutts, J. Lefaucheur, X. X. Zhang, P. Hong, M. Bass, I. A. Shesherbakov, and A. I. Zagumennyi, *OSA Proc. Adv. Solid-State Lasers* **20**, 41 (1994).
- ⁵G. Feugnet, C. Bussac, C. Larat, M. Schwarz, and J. P. Pocholle, *Opt. Lett.* **20**, 157 (1995).
- ⁶V. Lupei, A. Lupei, C. Tiseanu, S. Georgescu, C. Stoicescu, and P. M. Nanau, *Phys. Rev. B* **51**, 8 (1995).
- ⁷R. B. Barthem, R. Buisson, and J. C. Vial, *J. Phys. (France)* **46**, 483 (1985).
- ⁸R. B. Barthem, R. Buisson, J. C. Vial, and H. Harmand, *J. Lumin.* **34**, 295 (1986).
- ⁹F. S. Ermeneux, C. Goutaudier, R. Moncorge, M. T. Cohen-Adad, M. Bettinelli, and E. Cavalli, *Opt. Mater.* **13**, 193 (1999).
- ¹⁰O. Guillot-Noël, D. Simons, and D. Gourier, *J. Phys. Chem. Solids* **60**, 555 (1999).
- ¹¹O. Guillot-Noël, B. Viana, B. Bellamy, D. Gourier, G. B. Zogom-boulou, and S. Jandl, *Opt. Mater.* **13**, 427 (2000).
- ¹²W. M. Yen, V. Lupei, S. Georgescu, and C. Ionescu, *Rev. Roum. Phys.* **33**, 1007 (1988); R. B. Barthem, R. Buisson, and R. L. Cone, *J. Chem. Phys.* **91**, 627 (1989); R. B. Barthem, R. Buisson, F. Madéore, J. C. Vial, and J. P. Chaminade, *J. Phys. (France)* **48**, 379 (1987).
- ¹³M. Malinowski, *Phys. Rev. B* **34**, 7578 (1986).
- ¹⁴A. Lupei, V. Lupei, and S. Georgescu, *J. Phys.: Condens. Matter* **4**, L221 (1992).
- ¹⁵N. Pelletier-Allard, R. Pelletier, C. Tiseanu, and A. Lupei, *J. Lumin.* **62**, 61 (1994); C. Barthou and R. B. Barthem, *ibid.* **46**, 9 (1990).
- ¹⁶N. Pelletier-Allard and R. Pelletier, *J. Phys. (France)* **43**, 403 (1982).
- ¹⁷R. Buisson and J. Q. Liu, *J. Phys. (France)* **46**, 1523 (1984); R. Buisson, J. Q. Liu, and J. C. Vial, *ibid.* **45**, 1533 (1984).
- ¹⁸T. T. Basiev, V. V. Fedorov, A. Ya. Karasik, and K. K. Pukhov, *J. Lumin.* **81**, 189 (1999).
- ¹⁹C. L. M. de Barros, R. B. Barthem, and N. M. Khaidukov, *J. Lumin.* **82**, 307 (1999).
- ²⁰F. Ramaz, J. C. Vial, and R. M. Macfarlane, *J. Lumin.* **53**, 244 (1992).
- ²¹M. P. Hehlen, H. U. Gudel, Q. Shu, J. Rai, and S. C. Rand, *Phys. Rev. Lett.* **73**, 1103 (1994); M. P. Hehlen, A. Kuditcher, S. C. Rand, and S. R. Luthi, *ibid.* **82**, 3050 (1999); M. P. Hehlen, H. U. Gudel, Q. Shu, and S. C. Rand, *J. Chem. Phys.* **104**, 1232 (1996).
- ²²J. M. Clemens and C. A. Hutchison, Jr., *Phys. Rev. B* **28**, 50 (1983).
- ²³R. L. Cone and R. S. Meltzer, in *Spectroscopy of Solids Containing Rare Earth Ions*, edited by A. A. Kaplyanskii and R. M. Macfarlane (Elsevier Science, North-Holland, 1987), Vol. 21, Chap. 8, p. 481.
- ²⁴A. Bencini and D. Gatteschi, in *EPR of Exchange Coupled Systems* (Springer-Verlag, Berlin, 1989), p. 21.
- ²⁵R. L. Belford, N. D. Chasteen, H. So, and R. E. Tapscott, *J. Am. Chem. Soc.* **91**, 4675 (1969).
- ²⁶J. P. Sattler and J. Demarich, *Phys. Rev. B* **4**, 1 (1971).
- ²⁷O. Guillot-Noël, A. Kahn-Harari, B. Viana, D. Vivien, E. Antic-Fidancev, and P. Porcher, *J. Phys.: Condens. Matter* **10**, 6491 (1998).
- ²⁸V. V. Osiko, Yu. K. Voronko, and A. A. Sobol, in *Crystals* (Springer-Verlag, Berlin, 1984), Vol. 10, p. 37.